Iranian Journal of Science & Technology, Transaction B, Engineering, Vol. 29, No. B2
Printed in The Islamic Republic of Iran, 2005
© Shiraz University

FINITE ELEMENT, MODAL TESTING AND MODAL ANALYSIS OF A RADIAL FLOW IMPELLER[*]

S. ZIAEI RAD

Dept. of Mechanical Engineering, Isfahan University of Technology, Isfahan, I. R. of Iran
Email: szrad@cc.iut.ac.ir

Abstract– This paper is concerned with the finite element analysis and modal testing of an industrial radial flow impeller. The goal is to determine and verify the vibration characteristics of the impeller using both experimental and analytical techniques.

The finite element model of the impeller with tapered blades was built using a 3D solid element. The convergence properties of the FE model was then verified by mesh refinement and mass distribution methods. Next, a pre-test plan was performed before conducting a modal test in order to select the proper suspension points, driving point(s) and response points on the impeller.

Impact testing using hammer excitation and laser Doppler vibrometer (LDV) response measuring techniques were used to measure the vibration properties of the impeller. Using a scanning laser Doppler vibrometer enabled the backplate modes to be described in terms of their nodal diameter components. The nodal diameters versus natural frequencies graph was then compared with the same results obtained from FE and hammer testing and showed good agreement.

Finally, a parametric study was conducted on disc thickness, blade thickness, blade trailing, leading edge profiles and blade mistuning. It was found that the effect of varying disc thickness on the lower modes of the impeller was not significant. However, significant natural frequency shifts were observed for the higher modes. It was also concluded that varying the blade leading edge position had a marked effect on the natural frequencies while the lower modes were somehow insensitive to the variation of trailing edge position.

Keywords– Radial flow impeller, modal analysis, laser Doppler vibrometer, test planning, finite element

1. INTRODUCTION

Turbomachinery blades are usually exposed to very hostile operating conditions and failure of a single blade may lead to major secondary damage of the machine. This explains why the vibration characteristics of turbomachine blades have been studied in such great detail [1-2]. However, most investigations have dealt with axial-flow turbomachines rather than radial-flow ones [2]. This is mainly due to the fact that the former category has been used extensively in aircraft propulsion, which is perceived to be a more critical application. However, greater knowledge of the vibration behavior of radial-flow impellers will be useful for optimising their fatigue-life and efficiency, possibly resulting in increased performance and applicability.

The particular case study used for this paper was an industrial radial-flow impeller shown in Fig. 1. It is of the unshrouded single-entry type, forged in high-grade aluminium, with nineteen integral, radially-disposed, non-uniformly tapered blades. In general terms, the investigation has been divided into three main sections: 1-Finite element analysis, 2-Modal testing and modal analysis, and 3-Sensitivity analysis

The finite element method, which originated in the field of structural analysis, was widely developed and exploited in the aerospace industry during the 1960s and 1970s. Information on this and other advanced topics may be found in [3-7].

Due to a general lack of confidence in FE models, the dynamic testing of structures has become a standard procedure for model validation and updating [8]. Over the past thirty years, modal testing and analysis have become a fast-developing technique for the experimental evaluation of the dynamic properties of structures [8]. The experimental studies using modal analysis were mostly used to validate the FE results.

---

[*] Received by the editors October 19, 2003 and in final revised form September 26, 2004

Before a modal test is performed, there are some features that should be carefully selected [9]. In this way, the test can be carried out effectively as data from the test contain more useful information. Among these considerations, selecting suspension points, driving point(s) and response points are the most important, especially for a modal test for model validation [10].

Test planning is undertaken to help decide the optimum conditions for the test set-up. That is: to determine how and where to suspend the test structure, how to select the point(s) in the test structure for excitation, and how to choose the response DOFs to be measured. Sometimes all these choices can be made using the test engineer's experience or intuition. However, for a test structure with a complex shape and complex configuration, relying on experience and intuition is not enough to achieve the optimum conditions especially when encompassing a wide range of frequency.

2. THE FINITE ELEMENT MODELING OF RADIAL-FLOW IMPELLER

a) The finite element model

At the first stage, the impeller was modeled using 3D 20-noded brick elements. The constructed FE model consists of 14256 elements and 114048 DOFs (Fig. 2). Next, the subspace technique was used to extract the first 100 natural frequencies and mode shapes of the model. The extracted modes were then saved.

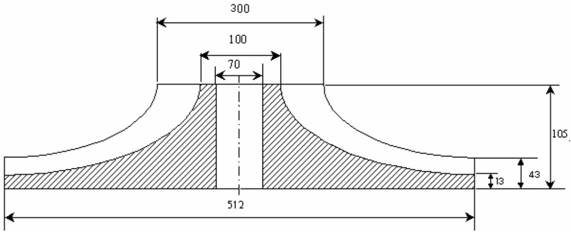

Fig. 1 Radial flow impeller (Dimension in mm)

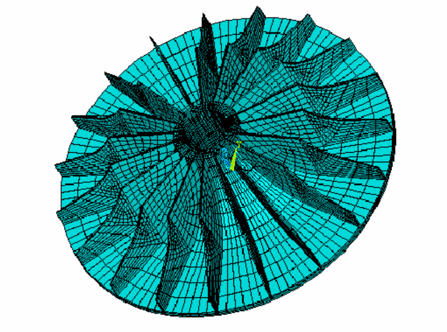

Fig. 2 Impeller mesh using solid element

Table 1 lists the results obtained for the impeller in a free-free condition (rigid-body modes were excluded), while some of the mode shapes are depicted in Fig. 3. The modal diameter for each mode was realized using visual inspection and fast Fourier transform (FFT) calculation of all nodes on the outer diameter of the impeller backplate.

Table 1. Natural frequencies and nodal diameter of the impeller

Mode No.	Natural frequency (Hz)	Nodal diameter
1,2	950.4	2
3,4	960.5	4
5,6	960.8	3
7,8	961.0	5
9,10	961.2	6
11,12	962.7	7
13,14	963.3	8
15,16	963.6	9
17,18	999.6	1
19	1011.6	0
20,21	1156.2	2
22,23	1649.7	3
24,25	1952.7	4
26	1986.5	0
27,28	2145.3	5
29,30	2207.5	6
31,32	2228.8	7

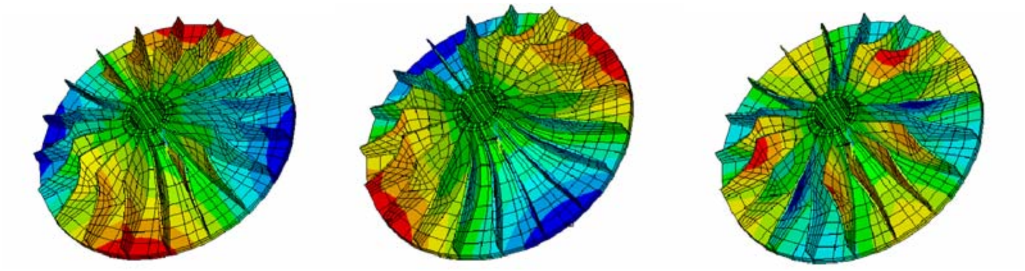

a- Mode shape 1 (2 ND) b- Mode shape 2 (2 ND) c- Mode shape 3 (4 ND)

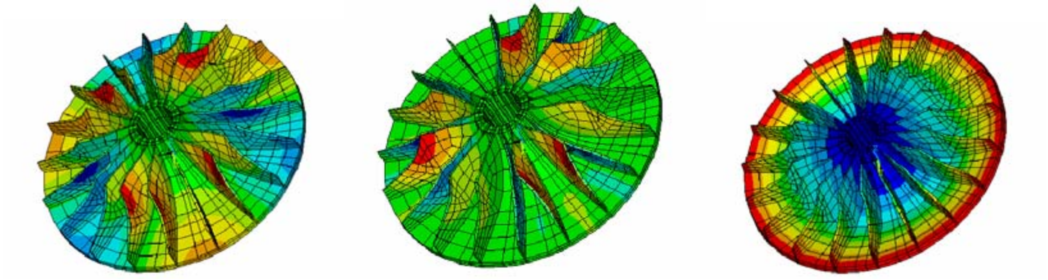

d- Mode shape 5 (3 ND) e- Mode shape 13 (8 ND) f- Mode shape 26 (0 ND)

Fig. 3. Mode shapes of the Impeller using solid elements

Figure 4 plots a graph of the impeller natural frequencies versus nodal diameters. Next, a Campbell diagram for the model in the operating range 0-18000 rev/min was calculated. The results are depicted in Fig. 5. To evaluate the effect of rotating speed on the natural frequency and mode shapes of the impeller, the rotating speed was increased by a step of 1000 rev/min and the first 100 modes were obtained and stored for later processing. It can be seen from the Campbell diagram that the maximum change in the natural frequencies is less than 15 percent in the impeller operating range.

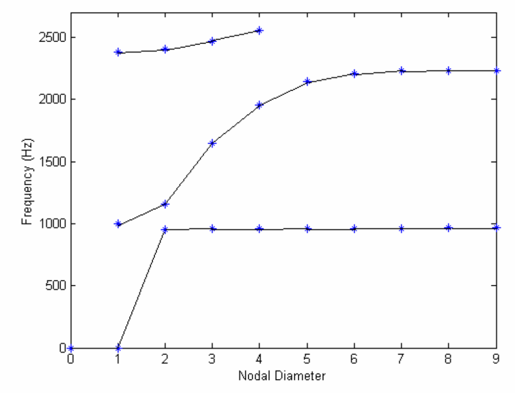

Fig. 4. Natural frequency versus nodal diameter

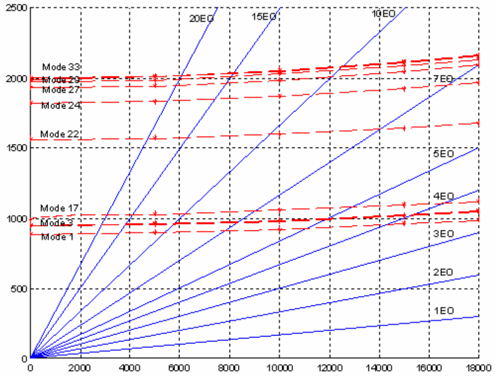

Fig. 5. The Campbell diagram for the impeller

b) FE model convergence

When an FE model is to be validated, the requirement on the convergence of the model must be satisfied. This means that the dynamic properties predicted by the model can be trusted in the frequency range of interest. In this study two techniques were used to determine the convergence range or the number of converged-predicted modes of the FE models.

The first technique is based on mesh refinement. Two different meshes are applied to the same structure where two modal data sets can be obtained. The natural frequency differences between the same modes of these two sets can then be used to determine the convergence frequency range or the number of converged modes. Figure 6 shows the natural frequency difference between the same modes when two different meshes were applied in the FE model of the impeller. It can be seen that for our model the difference is less than 1.5%, which is an acceptable threshold. In other words, the model has converged in the frequency range of interest, i.e., 0-2300 Hz.

In the second technique, two different mass distribution methods were applied for the normal mode solution of each FE model so that two modal data sets are obtained for each FE model. Again, the natural frequency differences between the corresponding modes of these two modal data sets can be used to determine the convergence frequency range of the FE model. One can propose a threshold of say 10% for the natural frequency difference of the same modes [11]. Plotting the natural frequency differences of the same modes predicted by the same FE model when using two mass distribution methods or fine and coarse meshes, one can identify the convergence frequency range or the number of converged predicted modes. Figure 7 shows the natural frequency differences between the same modes when the two mass distribution methods, namely consistent and lumped mass distributions, were applied. Two different mesh densities are used for each distribution, thus yielding four sets of results. It is clear from the graph that the finer the model, the smaller the natural frequency difference. The maximum difference in natural frequency, in the frequency range of interest (0-2300 Hz), for the model using solid elements is less than 6.2%.

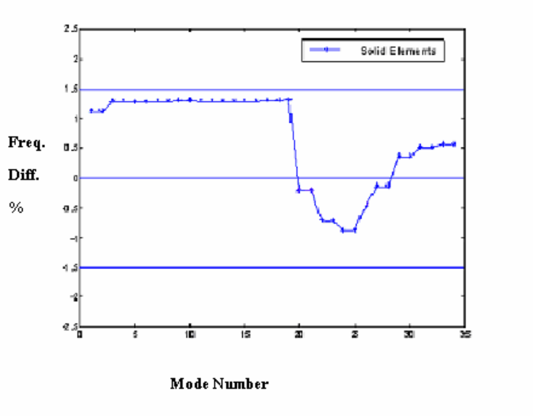

Fig. 6. Natural frequency difference with different mesh densities

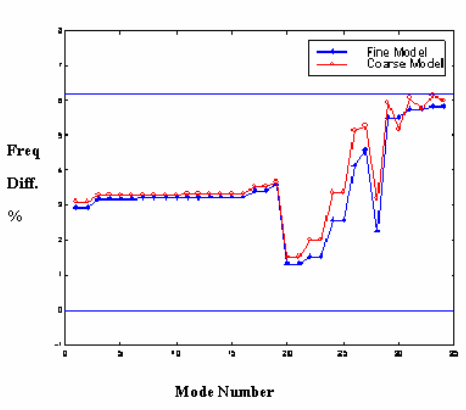

Fig. 7. Natural frequency difference between the same mesh with different mass distributions

3. MODAL TESTING

a) Pre-test planning

In order to ensure that the FE model of a structure can be used with confidence for the prediction of the dynamic behavior of that structure, the model must be validated by tests. In the validation process, several types of tests should be performed to obtain measured data, and then used for comparison with data predicted by the FE model.

Before a modal test is performed there are some features that should be carefully selected. Test planning is undertaken to help in deciding the optimum conditions for the test set-up. For the process of FE model validation, there must be an initial FE model. Although this model may not be reliable enough to predict the dynamic properties of the structure accurately, it must contain some useful information about the structure's dynamic properties. A test planning program was developed and used here based on the FE models developed earlier to give some guidance for test planning.

a-1. Optimum suspension point(s) selection: First, the suspension arrangements should be considered to make sure that the test structure is supported in the desired condition. In many modal tests, free-free conditions are required. However, providing such a condition in practice is difficult. Therefore, the suspension points in such a test should be selected so that the suspension has as little effect as possible on any mode of vibration in the frequency range of interest.

In most modal tests, relatively soft springs were used to connect the test structure to ground [8, 10, 12-13]. Thus, it can be assumed that there is no mass, but only stiffness attached to the suspension points so that any additional forces will result from displacement of the suspension points. The stiffness of the suspension should be as low as possible so that the natural frequency of the highest rigid-body mode of the test structure is well below the natural frequency of its first flexible mode [8, 10, 12-13]. In addition to this consideration, selecting the optimum suspension points can be helpful in reducing the additional forces to the test structure during the test.

The optimum suspension points can be selected on the basis of two criteria [14]. The first criterion is that the total displacement amplitude at all of the selected points for all modes in the specified frequency range be as low as possible, so that the additional forces caused by the displacement at these points during the test will be negligible. The second criterion is that the vibration movement at a suspension point during the test is mainly in a plane that is normal to the suspension spring axis. Of course, there are some other limitations for suspension points selection: for example, the points selected must be accessible and have no need to drill through the specimen or attach additional items.

Different parameters can be defined to satisfy the above conditions mathematically. The program was developed to calculate the magnitude of a parameter called "average driving point degree of freedom" (ADDOF) for each DOF in the FE model (Fig. 8). This parameter is then used to aid the selection of optimum suspension points [15].

a-2. Optimum driving point(s) selection: In a given frequency range, every mode of the test structure has a different mode shape and pattern of nodal lines. If the chosen driving point is in the vicinity of a nodal line of any individual mode, that mode cannot be excited to a sufficient level to ensure that the measurement of its properties will be reliable. Worse, a mode can be missed altogether if the driving point is located exactly on a nodal line of the mode.

Different excitation methods can also influence the selection of the driving point. If the hammer excitation method is to be used in a modal test, the vibration velocity amplitude at the driving point should not be so large as to give a high possibility of a double hit. If shakers are to be used to excite the test structure, the vibration acceleration amplitude at the driving point should be limited in order to eliminate the inertial effects caused by the additional mass of excitation equipment and force sensor(s).

The optimum driving point(s) selection process in the developed program is based on two criteria. The first criterion is to avoid selecting a point near to any nodal line of any of the modes in the specified frequency range. The second criterion is to avoid selecting the points with an excessively large vibration amplitude.

In the program, two parameters have been developed to help select the optimum driving points: the optimum driving point (ODP), and the non-optimum driving point (NODP) quantities. The ODP (Fig. 9) indicates where the points may be selected as driving points, while the NODP indicates points which should not be selected as driving points. Combining the ADDOF parameters with these two, ODP-based and NODP-based criteria can be used to help select points that fulfill both criteria for selecting the optimum driving points.

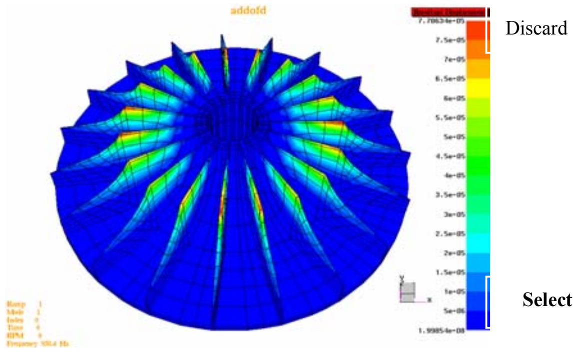

Fig. 8. ADDOFD plot for the impeller

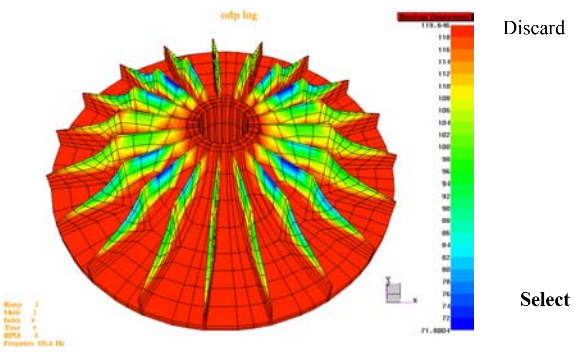

Fig. 9 ODP plot for the impeller

a-3. Optimum response DOFs selection: In a model validation process, the measured data should contain sufficient information to positively identify each mode in the specified frequency range. That means that all measured modes should be linearly independent at DOFs where the response is measured. In pursuit of obtaining accurate measurements, the DOFs with large vibration amplitudes are usually preferred for measurement. On the other hand, the number of measurements cannot be enlarged without reaching practical limits. In order to fulfill both of these requirements, the response DOFs should be selected so that they contain enough information to distinguish all the modes, while at same time the number of measurements should be kept as low as possible (less than 5% of total model DOFs).

The effective independence (EI) method in the test planning program is used to provide information on the contribution of each DOF to the global independence of the mode shapes [15]. By using the ADDOF-EI method [16-17] (a combination of the ADDOF parameters and the EI criterion), information can be provided by combining the results from an EI calculation with the vibration amplitude at each DOF (Fig. 10). According to the information from each of these methods, the user can employ the functions to remove those DOFs with less contribution to the global independence and/or with lower vibration amplitudes. In this way, the program gives a list of DOFs that can be used as response DOFs for measuring in the modal test, indicating the relative priority of each. Again, there are practical limitations for using the selected points, such as accessibility.

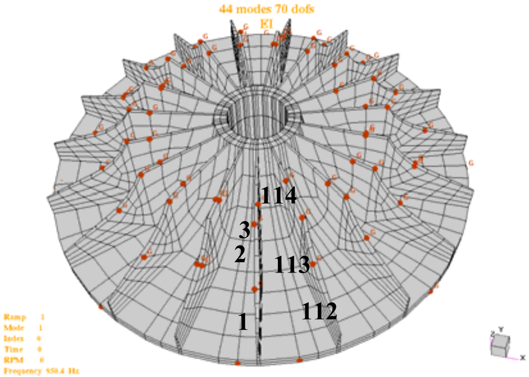

Fig. 10. ADDOF-EI plot for the impeller (44 modes and 77 DOFs)

Here, 114 points were selected as measurement locations, 76 being provided by the algorithm and 38 being added for a better visualisation of the mode shapes.

b) Modal testing and modal analysis

b-1. Hammer testing: The impeller was suspended by three soft springs and tested in a free-free condition. The best suspension points were selected from the pre-test plan. The experimental data were obtained via hammer testing using a B&K 2032 analyser connected to a PC. One B&K piezoelectric accelerometer (Endevco. 2222c) was attached to point 1 on the structure by using wax (Fig. 10). A total of 114 response points were selected via the procedure explained in section 3.1. The measurements were carried out by impacting the structure at point 1 and acquiring the response data at points 1 to 114. The measured points around the impeller are shown in Fig. 10. The frequency response functions (FRFs) were measured in three different windows, namely; 800-1600Hz, 1600-2400Hz and 2400-3200Hz. The measured FRFs for half of the points were in the z-direction (1, 2, 3, 7, 8, 9, 13, 14, 15 … 109, 110, 111), while for the other half were in the θ direction (4, 5, 6, 10, 11, 12, 16, 17, 18 … 112, 113, 114). Typical measured FRFs for points 1 and 4 are plotted in Fig. 11.

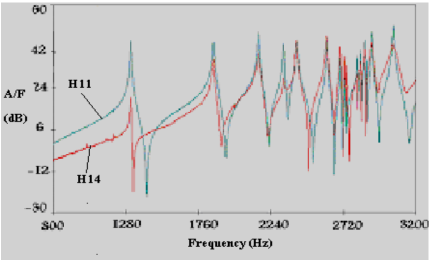

Fig. 11. Overlay of FRFs H_{11} (Z-direction, Blue) and H_{14} (θ-direction, Red) of the impeller

b-2. Modal analysis procedure: In the second stage, the experimental FRF data were analyzed using a global multi-FRF analysis method [8]. The technique is based on a complex singular value decomposition of a system matrix expressed in terms of measured FRFs, and then on a complex eigensolution which extracts the required modal properties [8, 18]. This particular algorithm was chosen because of its ability to detect close modes. The data were analyzed by applying 3 runs on each of several frequency windows, thus covering the entire frequency range. The most consistent results were saved in a modal data set.

Table 2 presents the measured natural frequencies for the impeller versus calculated results from FE models. Natural frequency differences between measured and FE predicted results are also included. The results from the FE model using solid elements are in good agreement with the modal testing data within the investigated region (error less than 16%). Slight discrepancies may be accounted for geometric and material approximations made during the creation of the FE model. However, the MAC values [8, 19] comparing experimental and FE models using modes with the same number of nodal diameters and nodal circles were poor. This can be explained by the fact that modes were very close and need higher frequency resolution and more measured points to express them more accurately. Instead, it was decided to compare a plot of natural frequency versus the number of nodal diameters for the measured and predicted data.

Table 2. Natural frequency results for the impeller (Measured against FE)

Measurement			Finite element		Difference
Natural frequency (Hz)	Nodal diameters	Damping %	Natural frequency (Hz)	Nodal diameters	Natural frequency (%)
957.0	2	0.31	950.4	2	0.7
965.5	9	0.99	963.6	9	0.2
969.9	9	0.34	963.6	9	0.7
1004.8	1	0.40	999.6	1	0.5
1024.2	1	0.21	999.6	1	2.4
1151.9	2	0.10	1156.2	2	-0.4
1197.3	2	0.07	1156.2	2	3.4
1311.5	2	0.36	Not Predicted	-	-
1312.6	2	0.30	Not Predicted	-	-
1859.8	3	0.34	1649.7	3	11.3
1862.9	3	0.43	1649.7	3	11.4
2156.9	4	0.37	1952.7	4	9.5
2159.0	4	0.29	1952.7	4	9.6
2323.4	5	0.27	2145.3	5	7.7
2324.5	5	0.41	2145.3	5	7.7
2410.9	5	0.39	Not Predicted	-	-
2610.7	6	0.42	2207.5	6	15.4
2612.2	7	0.13	2228.8	7	14.7
2613.2	7	0.23	2228.8	7	14.7

b-3. Laser Doppler Vibrometer (LDV) measurements: A complete characterization of the mode shapes of an impeller may require a total displacement/velocity/acceleration field measurement such as holography. But for many bladed-disk applications, a circular line scan near the periphery can be very effective, enabling the backplate mode to be described in terms of its nodal diameter components. This can also help to verify the results obtained by the hammer testing.

The report by Ziaei Rad and Stanbridge [20] covers some measurements on the same impeller as a demonstration of the circumferential line scan technique using a laser Doppler vibrometer (LDV) [21]. In this paper, we are not going to explain details of the technique used. However, the results from the LDV measurements will be compared with those of impact testing and finite elements. Interested readers are referred to the articles [20-23].

The Ometron VPI LDV was first aligned with the impeller axis, and its X-Y mirrors supplied with suitably-phased sinusoidal inputs to cause the beam to circle the impeller backplate at 20 Hz just inside its outer balancing rim. With this set-up the scanning beam measures in a cone with the measurement axis being inclined to the perpendicular. The LDV was approximately 2m far from the impeller surface, assuming vibration to be perpendicular to the surface, the LDV measured 99.8% of the true amplitude (Fig. 12).

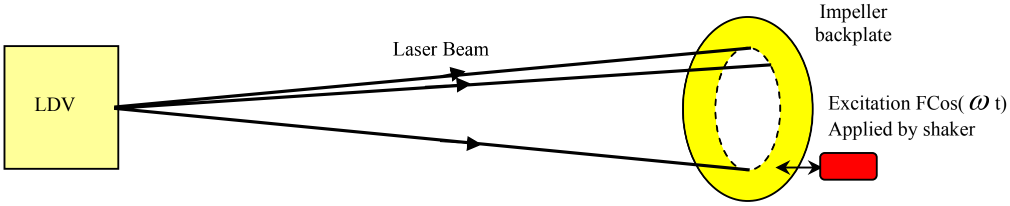

Fig. 12 Scanning laser Doppler vibrometer applied to impeller backplate

The impeller was next excited at each natural frequency by supplying a sine wave to the shaker at the frequency indicated from a peak on the FRF. The LDV signal output was analyzed by a zoom FFT centered near to the natural frequency and its spectrum recorded. A 1kHz 500-point transform was used in each case, with a flap-top window. The frequency range covered the first two families of modes. Figure 13 shows LDV spectra was obtained in this way at response peaks for some frequencies.

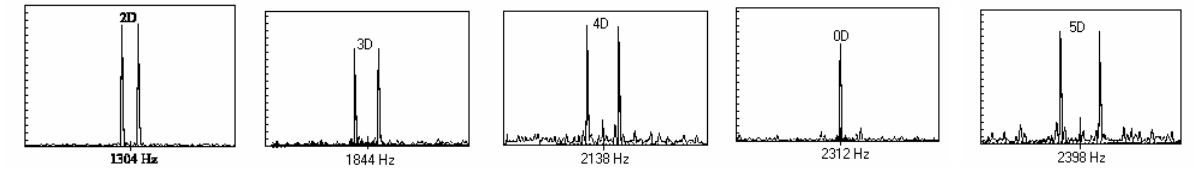

Fig. 13. Rotating LDV measured response spectra at natural frequencies

Next, the impeller response at any given excitation frequency was defined by spatial Fourier coefficients of the circumferential response, i.e. by sine and cosine terms (or magnitude and phase) corresponding to 0, 1, 2, etc. nodal diameter. These nodal diameters then can be plotted as a function of excitation frequency. These, together with the results from hammer testing and FE analysis are compared in the next section.

b-4. Correlation of experimental and predicted results: Figure 14 compares the natural frequency versus the nodal diameter results obtained from the predicted FE, LDV and hammer testing measurements. The LDV and hammer testing results are in good agreement and for both cases the measured natural frequencies are higher than those predicted by FEM. It is also not possible to measure all nodal diameter modes, especially if they are clustered in a high modal density using LDV or hammer testing. For example, there are 8 pairs of modes in the frequency range of 960 to 980 Hz.

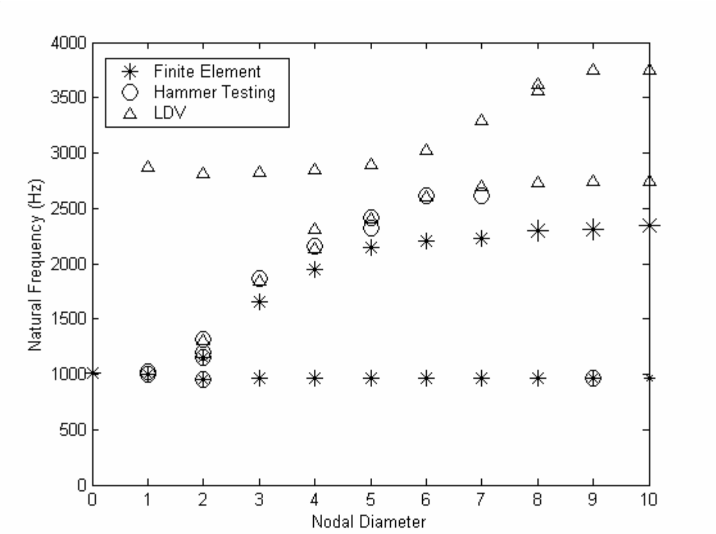

Fig. 14. Comparison of natural frequencies versus nodal diameters for LDV, hammer testing, FE

4. SENSITIVITY ANALYSIS

Having finished the measurement and finite element validation, it was decided to accept the initial finite element model without any correction or model updating on it. One also can apply some correction to the FE model in order to improve its dynamics properties either by finite element updating techniques [24-29], or by trial and error. An investigation was carried out in this section to calculate the sensitivity of radial-flow impeller modes to different parameters such as disc thickness, blade thickness, blade trailing, and leading profiles and blade mistuning. Such a sensitivity analysis is necessary for design stages of the impeller.

a) Effect of varying disc thickness

The first parametric study was devoted to the disc back plate thickness. For this case, the disc thickness was changed from 0.2 to 4 times the normal thickness. It was found that the variation is not significant for the lower modes. However, significant shifts in the natural frequencies were observed in higher modes. The maximum variation in natural frequency is around 38 percent for modes in the frequency range of 1400 to 1600Hz.

b) Effect of varying blade thickness

The parametric study of natural frequency variation versus blade thickness showed that the relationship is virtually proportional for the low frequency range, while there is a slight frequency decrease for modes above 2200Hz. The modes with natural frequencies of 1150 and 1634 Hz are almost insensitive to the variation of blade thickness, 0.4% for these modes compared with 5% for the first mode.

c) Effect of varying blade trailing edge profile

Figure 15 shows the section of blade which is used for the trailing edge parametric study. The parametric study on the trailing edge profile was conducted to see how this parameter affects the dominant modes of the impeller. The results indicate that modes below 1400 Hz are almost completely insensitive to a variation of this parameter. The greatest variation for the lowest mode (1153.9 Hz) of the tested configuration was less than 1.3%. However, the greatest variation in the frequencies is above 30%, and that is for mode 40 at 2250 Hz.

d) Effect of varying blade leading edge profile

Figure 16 shows the section of a blade which is used for the leading edge parametric study. The results show that the lower modes are the most sensitive ones for this case. It was found that the natural frequencies of the lower modes decrease by increasing the x_0 parameter in Fig. 16, while the situation is almost reversed for the higher modes. The natural frequency variation was between 27 to 40% for the lower modes, while the maximum variation for the higher modes is less than 5%.

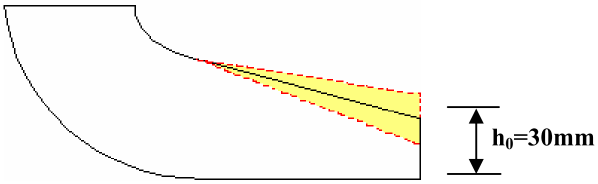

Fig. 15. Variation of blade trailing edge profile study

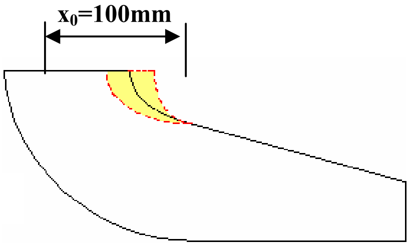

Fig. 16. Variation of blade leading edge profile study

e) Effect of mistuning a blade

The effect of mistuning due to slight discrepancies in blade geometry has been studied in depth by many researchers [30-32]. In this study, the modulus of elasticity of one of the impeller blades was changed between 0 and 11% of the nominal value and the first 40 natural frequencies of the impeller were calculated using a finite element. Figure 17 shows the effect of mistuning on the natural frequencies of the impeller. It can be seen that blade natural frequencies were not heavily affected by this parameter. The maximum change in the blade frequency for this case is less than 2.5%.

The effect of mistuning a blade on the mode shapes of the impeller is, however, more dramatic. The mode shapes are no longer simply 2ND, 3ND, 4ND,… modes, but they are a combination of all these nodal diameter components (3D plots are not shown). A Fourier transform of each mistuned mode shape reveals that several other harmonics are present (Fig. 18). This is a significant observation for forced response analysis, as such modes are far more likely to be excited by some general unsteadiness.

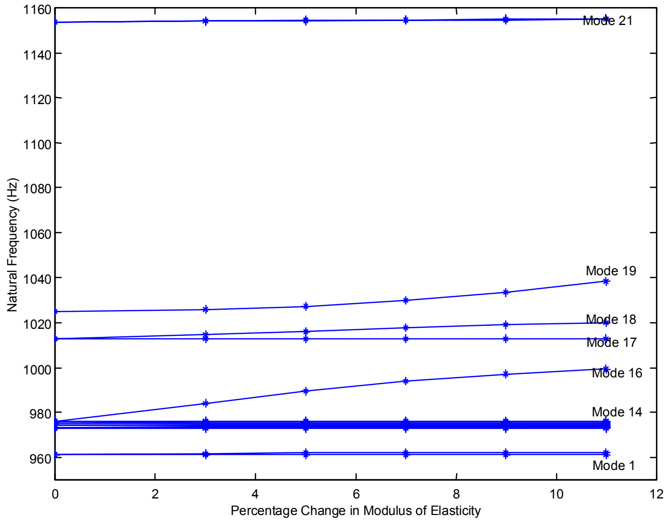

Fig. 17. Effect of one blade mistuning on impeller modes

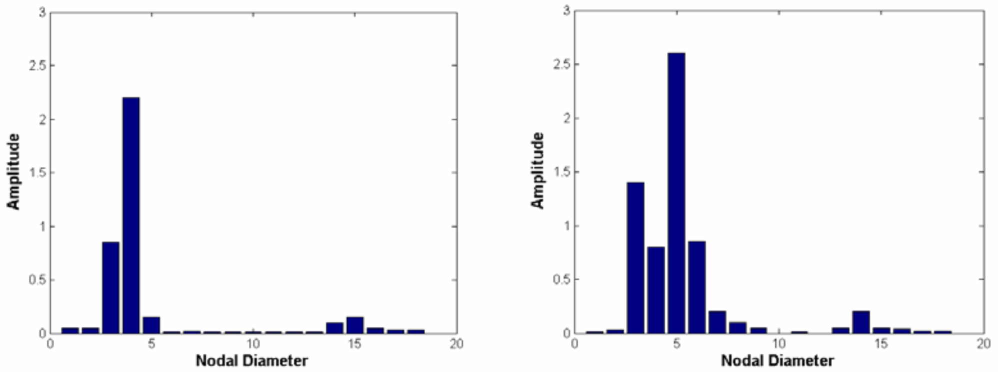

a- Mode shape no. 3

b- Mode shape no. 8

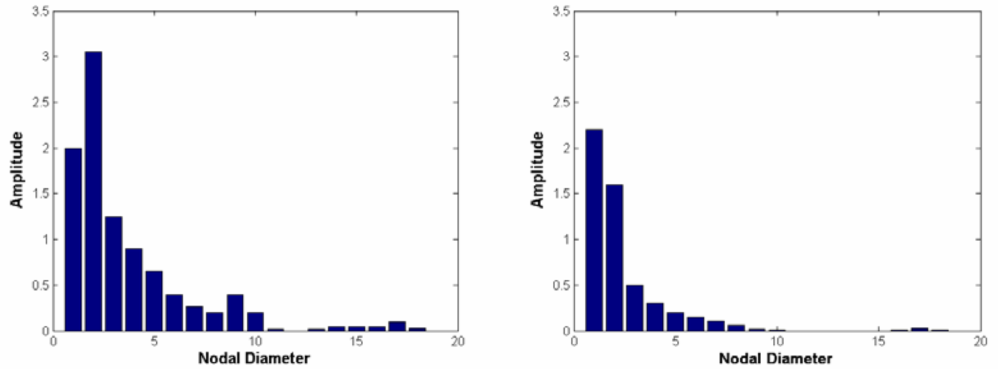

a- Mode shape no. 16

b- Mode shape no. 18

Fig. 18. Fourier components of impeller's mode shapes with blade mistuning

Finally, Table 3 shows the sensitivities of the first 34 flexible modes of the impeller to small changes in the parameters studied in the previous sections. In order to calculate these sensitivities, each parameter was increased first by one percent, then decreased by one percent and the changes in the natural frequencies was calculated and multiplied by 100 to find the final sensitivity values in %, that is

$$\begin{aligned} Sensitivity_i^+ &= \frac{Natural\ Frequency_i(p+\Delta p) - Natural\ Frequency_i(p)}{Natural\ Frequency_i(p)} \times 100 \\ Sensitivity_i^- &= \frac{Natural\ Frequency_i(p) - Natural\ Frequency_i(p-\Delta p)}{Natural\ Frequency_i(p)} \times 100 \\ Sensitivity_i &= \frac{Sensitivity_i^+ + Sensitivity_i^-}{2} \end{aligned} \tag{1}$$

p is the parameter (blade thickness, …), Δp is the change made to the parameter and i is the mode number.

Table 3. Sensitivity of impeller natural frequencies with respect to different parameters

Mode number	Natural frequency (Hz)	Nodal diameter	Disc thickness sensitivity %	Blade thickness sensitivity %	Blade trailing edge sensitivity %	Blade leading edge sensitivity %
1,2	950.4	2	0.0063	0.0683	-0.0039	0.8498
3,4	960.6	4	0.0244	0.0855	-0.0017	0.9420
5,6	960.9	3	0.0186	0.0853	-0.0018	0.9365
7,8	961.0	5	0.0288	0.0860	-0.0016	0.9450
9,10	961.9	6	0.0307	0.0867	-0.0015	0.9464
11,12	962.7	7	0.0310	0.0875	-0.0014	0.9467
13,14	963.3	8	0.0308	0.0880	-0.0013	0.9467
15,16	963.6	9	0.0306	0.0883	-0.0013	0.9466
17,18	999.57	1	-0.0024	0.0999	0.0002	0.9165
19	1011.6	0	-0.0203	0.1084	0.0018	0.8786
20,21	1156.2	2	-0.1130	0.0090	-0.0123	0.0595
22,23	1649.7	3	-0.0465	0.0033	-0.0212	-0.1084
24,25	1952.7	4	0.1024	-0.0041	-0.0450	-0.1278
26	2142.4	0	-0.0827	0.0199	-0.0092	-0.1462
27,28	2145.3	5	0.1581	-0.0283	-0.0972	-0.0588
29,30	2207.5	6	0.1082	-0.0347	-0.1144	0.0118
31,32	2228.8	7	0.0831	-0.0340	-0.1152	0.0375
33,34	2238.2	8	0.0721	-0.0331	-0.1144	0.0477

Fig. 19 shows the sensitivity of impeller natural frequencies with respect to disc thickness, blade thickness, TE profile and LE profile. It is clear from the plot that for the lower modes, up to mode 20 (1153 Hz), the parameter ranking is (i) the leading edge profile, (ii) blade thickness, (iii) disc thickness and (iv) trailing edge profile, respectively. For modes higher than 1200 Hz, all parameters produce the same effect for comparable % change. For these higher modes, the disc thickness has the maximum sensitivity, while the trailing edge profile has the minimum one.

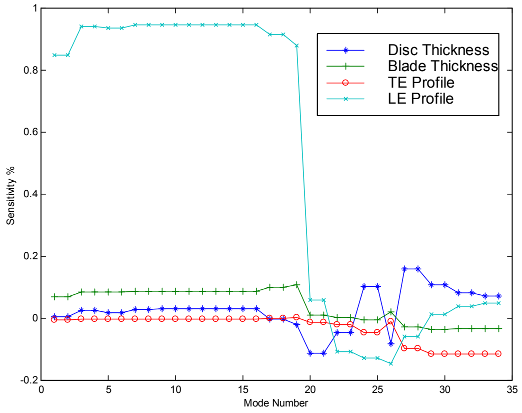

Fig. 19 Sensitivity of impeller natural frequencies respect to different parameters

5. CONCLUSIONS

An investigation has been carried out to examine in detail the vibration characteristics of a typical radial-flow impeller with a tapered blade. A solid element model was built and its convergence was verified by applying two mass distribution methods-lumped and consistent mass contribution-to each of the FE models and comparing the differences between the predicted natural frequencies in the two data sets.

Test planning was undertaken to find the optimum conditions for the test set-up. That is: to determine how and where to suspend the test structure, how to select the excitation point(s) in the structure, and how to choose the response DOFs to be measured.

Considering the measurement made, the results were satisfactory. Next, the modal analysis was carried out on the hammer testing results. The results show good agreement between the FE model using solid elements and measured natural frequencies. However, some modes have not accurately predicted the constant blade thickness used by FE model.

The measurements on the impeller as a demonstration of the circumferential line scan technique using a laser Doppler vibrometer (LDV) was also carried out, enabling the backplate mode to be described in terms of its nodal diameter components. The nodal diameter versus natural frequencies graph obtained from FE and hammer testing was compared and showed good agreement.

A parametric study was conducted on disc thickness, blade thickness, blade trailing and leading profiles, and blade mistuning. It was found that:

(i) The effect of varying disc thickness on the lower modes of the impeller was not significant. However, a significant shift in the natural frequencies resulted in higher modes.
(ii) The parametric study of natural frequencies versus blade thickness showed that the relationship is virtually proportional for the low frequency range, while for the higher modes it shows some decline.
(iii) The results from varying blade trailing edge profiles confirmed that first modes are nearly insensitive to the variation of this parameter. However, variation up to 40% can be seen for the higher modes.
(iv) It was concluded that the blade leading edge profile has a substantial effect on modal frequencies.
(v) Perturbing the modulus of elasticity of one of the impeller blades carried out for mistuning prediction. It was concluded that blade modes were not strongly affected by this parameter. The maximum change in the blade frequency for this case is less than 2.5%. However, the mode shapes were changed dramatically and they are no longer 2ND, 3ND, … modes. Instead they are a combination of these modes.

REFERENCES

1. Rao, J. S. (1991). *Turbomachine blade vibration*. New York: John Wiley & Sons.
2. Choi, S. T. & Chou,Y. T. (2001). Vibration analysis of elastically supported turbomachinery blades by the modified differential quadrature method. *Journal of Sound and Vibration, 240*(5), 937-953.
3. Zienkiewicz, O. C. (1971). *The finite element method in engineering science*. McGraw Hill.
4. Zienkiewicz, O. C. & Taylor, R. L. (1989). *The finite element method*. McGraw Hill.
5. Desai, C. S. & Abel, J. F. (1972). *Introduction to the finite element method*. Van Nostrand Reinhold, New York.
6. Nath, B. (1974). *Fundamental of finite elements for engineers*. Athlone Press, London.
7. Bathe, K. J. (1982). *Finite element procedures in engineering analysis*. Prentice-Hall, Englewood Cliffs, New Jersey.
8. Ewins, D. J. (2001). *Modal testing: theory and practice*. Research Studies Press.
9. Handbook on modal testing. (1993) Dynamic Testing Agency (DTA).
10. *Primer on best practice in dynamic testing*. (2000). Dynamic Testing Agency (DTA).
11. Chen, G. (1998). *The influence of mass distribution of NASTRAN FE Model*. Report No. VUTC/E2/98007, Centre of Vibration Engineering, Department of Mechanical Engineering, Imperial College, London.
12. Maia, N., Silva, J., He, J., Lieven, N., Lin, R., Skingle, G., To, W., Urgueira, A. (1997). *Theoretical and experimental modal analysis*. Research Studies Press Ltd.
13. Heylen, W., Lammens, S. & Sas, P. (1998). *Modal analysis theory and testing*. KUL, Belgium.

14. Imamovic, N. (1998). Validation Of large structural dynamics models using modal test data. PhD Thesis, Imperial College, University of London.
15. Imamovic, N., (1996). An automatic correlation procedure for structural dynamics. Rolls-Royce Report No. VUTC/E2/95006.
16. Imamovic, N. (1995). Methods for selection of measurement points for modal testing–average driving point residue (ADPR) method. Rolls-Royce Report No. VUTC/E2/95007.
17. Imamovic, N. (1996). Methods for selection of measurement DOF for modal testing–effective independence (EI) method and ADPR-EI method. Rolls-Royce Report No. VUTC/E2/96002.
18. Imregun, M. & Ewins, D. J. (1995). Complex modes-origins and limits. 13th IMAC, Nashville, Tennessee.
19. Allemang, R. J. & Brown, D. L. (1982). A correlation coefficient for modal vector analysis. *Proc. of the 1st Int. Modal Analysis Conf.*, 110-116.
20. Ziaei Rad, S. & Stanbridge, A. B. (1998). Modal tests on a centrifugal impeller. Centre of Vibration Engineering, Imperial College, Reprot No. VUTC/D/98010.
21. Ziaei Rad, S. & Ewins, D. J. (2000). Measuring RDOFs using laser Doppler vibrometer. *Tools for Noise and Vibration Analysis, Proc. of ISMA 25*, Leuven, Belgium.
22. Martarelli, M., Revel, G. & Santolini, C. (2000). Automated modal analysis by scanning laser vibrometry: problems and uncertainties associated with the scanning system calibration. *Mechanical Systems And Signal Processing, 15*(3), 581-601.
23. Halliwell, N. A. (1992). Vibration measurement using laser technology. Course Note, Section A, Loughborough University.
24. Lin, R. M. & Ewins, D. J. (1990). Model updating using FRF data. *15th International Modal Analysis Seminar*, K U Leuven, Belgium, 141-163.
25. Mottershead, J. E. & Friswell, M. I. (1993). Model updating in structural dynamics: A survey. *Journal of Sound and Vibration, 167*(2).
26. Ziaei Rad, S. & Imregun, M. (1996). *A modified eigenstructure assignment technique for finite element model updating. Journal of Shock and Vibration*, 247-258.
27. Ziaei Rad, S. & Imregun, M. (1996). On the accuracy required of experimental data for finite element model updating. *Journal of Sound and Vibration*. 323-336.
28. Ziaei Rad, S. & Imregun, M. (1996). Use of generic elements for model updating. *Tools for Noise and Vibration Analysis, Proc. of ISMA 21*, 1895-1906.
29. Ziaei Rad, S. & Imregun, M. (1999). On the use of regularisation techniques for finite element model updating. *Inverse Problems in Engineering, 7*, 471-503.
30. Ewins, D. J. (1975). Vibration modes of mistuned bladed discs. *Journal of Engineering for Power, Trans. ASME*, 349-355.
31. Ewins, D. J. (1980). Further studies of bladed disc vibration: Effect of packetting. *ImechE Conference, Cambridge*, 97-102.
32. Ewins, D. J. & Imregun, M. (1983). Vibration modes of packeted bladed discs. *Trans ASME, 106*, 175-180.